RESEARCH

Critical role for the Tsc1-mTORC1 pathway in β-cell mass in Pdx1-deficient mice

Juan Sun[1], **Liqun Mao**[1], **Hongyan Yang**[2] and **Decheng Ren**[1,2]

[1]Department of Medicine, The University of Chicago, Chicago, Illinois, USA
[2]Department of Gynecology, Key Research Laboratory of Gynecology, Guangzhou University of Traditional Chinese Medicine, Guangzhou, Guangdong, China

Correspondence should be addressed to D Ren: decheng@uchicago.edu

Abstract

Mutations in the pancreatic duodenal homeobox (*PDX1*) gene are associated with diabetes in humans. *Pdx1*-haploinsufficient mice also develop diabetes, but the molecular mechanism is unknown. To this end, we knocked down *Pdx1* gene expression in mouse MIN6 insulinoma cells. Pdx1 suppression not only increased apoptotic cell death but also decreased cell proliferation, which was associated with a decrease in activity of mechanistic target of rapamycin complex 1 (mTORC1). We found that in *Pdx1*-deficient mice, tuberous sclerosis 1 (*Tsc1*) ablation in pancreatic β-cells restores β-cell mass, increases β-cell proliferation and size, decreases the number of TUNEL-positive cells and restores glucose tolerance after glucose challenge. In addition, *Tsc1* ablation in pancreatic β-cells increases phosphorylation of initiation factor 4E-binding protein 1 (4E-BP1) phosphorylation and 40S ribosomal protein S6, two downstream targets of mTORC1 indicating that Tsc1 mediates mTORC1 downregulation induced by Pdx1 suppression. These results suggest that the Tsc1-mTORC1 pathway plays an important role in mediating the decrease in β-cell proliferation and growth and the reduction in β-cell mass that occurs in Pdx1-deficient diabetes. Thus, mTORC1 may be target for therapeutic interventions in diabetes associated with reductions in β-cell mass.

Key Words

- Tsc1
- mTORC1
- Pdx1
- β-cells
- β-cell mass

Journal of Endocrinology (2018) **238**, 151–163

Introduction

A decrease in pancreatic β-cell mass is associated with diabetes mellitus. Patients with type 1 diabetes have a dramatic reduction in β-cell mass, leading to insulin insufficiency and hyperglycemia. In type 2 diabetes, insulin resistance causes a compensatory expansion of β-cells and increased plasma insulin levels (Uchizono *et al.* 2009, Feng *et al.* 2016). However, diabetes eventually develops as β-cell mass decreases. Therefore, approaches to increase functional pancreatic β-cell mass may lead to improved therapeutic options for diabetes treatment. β-cell death, β-cell size and β-cell proliferation are the three major mechanisms to regulate pancreatic β-cell mass. β-cell replication maintains functional β-cell mass in adult mice and humans (Dor *et al.* 2004, Meier *et al.* 2008). Although several studies have shown primary effects on β-cell proliferation and growth following a variety of genetic or pharmacologic interventions (Bonner-Weir *et al.* 2010, Fiaschi-Taesch *et al.* 2010, Fiaschi-Taesch *et al.* 2013), the molecular mechanism underlying β-cell proliferation and growth need further clarification.

The mammalian target of rapamycin (mTOR), a serine/threonine kinase, is a master regulator of cellular metabolism and promotes cell size in response to environmental stimuli. mTOR forms two distinct signaling

http://joe.endocrinology-journals.org
https://doi.org/10.1530/JOE-18-0015

complexes, mTOR complex 1 (mTORC1, rapamycin sensitive) and mTOR complex 2 (mTORC2, rapamycin insensitive), by binding with multiple companion proteins such as mLST8, Tti1/Tel2, DEPTOR, RAPTOR and PRAS40 (Lee *et al.* 2007). mTORC1 integrates various stimuli and signaling networks to stimulate synthesis of protein, lipid and nucleotides and block catabolic processes such as autophagy at the post-translational and transcriptional levels (Jewell & Guan 2013, Shimobayashi & Hall 2014). The growth factor/PI3K/AKT signaling pathway is involved in regulating both mTORC1 and mTORC2. The tuberous sclerosis (TSC) tumor suppressor complex (TSC1/TSC2) is the most important upstream negative regulator of mTORC1. Activated AKT directly phosphorylates and inhibits TSC1/2 (Huang & Manning 2008). AKT-dependent phosphorylation results in dissociation of TSC1/2 from the lysosome, where the Ras homolog enriched in brain (Rheb) is localized, promoting Rheb activation. Since GTP-bound Rheb is a potent mTORC1 activator, inhibition of TSC1/2 by AKT-dependent phosphorylation results in mTORC1 activation (Kim & Guan 2015). Rapamycin not only inhibits β-cell proliferation *in vitro* but also blocks the effects of glucose and AKT activation on β-cell mass and proliferation by inhibition of mTOR in β-cells (Balcazar *et al.* 2009, Blandino-Rosano *et al.* 2012). Mice lacking *Tsc1* in pancreatic β-cells (*Rip-Tsc1* KO mice) develop obesity due to hypothalamic *Tsc1* excision in older *Rip-Tsc1*cKO animals, but young animals displayed a prominent gain-of-function β-cell phenotype prior to the onset of obesity. The young *Rip-Tsc1*KO animals displayed improved glucose tolerance due to mTOR-mediated enhancement of β-cell size, mass and insulin production (Mori *et al.* 2009*a*,*b*).

Pdx1 (pancreas and duodenal homeobox-1) plays an essential role in pancreas development, β-cell function and survival. Islet-specific disruption of *Pdx1* causes impaired insulin release, glucose intolerance and diabetes (Ahlgren *et al.* 1998, Johnson *et al.* 2003). Humans with heterozygous missense and frame shift mutations of the *Pdx1* gene develop reductions in insulin secretion resulting in one form of maturity-onset diabetes of the young (MODY 4). Previous studies from our laboratory and others have shown that islets from heterozygous $Pdx1^{+/-}$ mice are reduced in number, smaller in size and show increased susceptibility to cell death (Fujimoto *et al.* 2010*a*,*b*, Ren *et al.* 2014*a*). The present study was undertaken to determine whether mTORC1 plays a role in mediating pancreatic β-cell proliferation and growth in $Pdx1^{+/-}$ mice.

Materials and methods

MIN6 cell culture, quantification of mRNA levels and lentivirus-mediated shRNA expression

MIN6 cell culture, RNA isolation and first-strand cDNA synthesis and preparation of pLKO.1-Pdx1 shRNA lentivirus were performed as previously described (Ren *et al.* 2014*a*). TaqMan assay numbers were Hmbs, Mm00660262; Pdx1, Mm00435565; Tsc1, Mm00452208_m1 and Tsc2, Mm00442004_m1. Lentivirus was added to the medium on day 1. The blots were probed with antibodies against Pdx1 (07-696; Millipore), α-tubulin (T6199, Sigma), Actin (A-3853; Sigma), Tsc1 (6935; Cell Signaling), Tsc2 (4308, Cell Signaling), Phospho-S6 ribosomal protein (Ser240/244) (5364, Cell Signaling), S6 ribosomal protein (2217, Cell Signaling), 4E-BP1 (9644, Cell Signaling) and Phospho-4E-BP1 (Ser65) (9451, Cell Signaling), Phospho-AKT(Thr308) and Phospho-AKT (Ser473) (9916, Cell Signaling Sampler Kit), Phospho-GSK3β (Ser9) (9322, Cell Signaling) and GSK3β (9315, Cell Signaling). Phospho-S6 ribosomal protein blocking peptide is from Cell Signaling Technology (1220). Antibody detection was accomplished using enhanced chemiluminescence (PerkinElmer) and LAS-3000 Imaging system (FUJIFILM). The integrated density of each band was measured using NIH ImageJ software (Bethesda, MD, USA).

Immunofluorescence (IFC) and immunohistochemistry (IHC)

Pancreas tissue was harvested following transcardiac perfusion with 4% paraformaldehyde and fixed in 4% paraformaldehyde. Pancreatic sections were stained with antibodies against insulin and glucagon, phosphorylated S6 (p-S6; $Ser^{235/236}$ for immunohistochemistry (IHC) and immunofluorescence (IFC), Cell Signaling). Nascent protein synthesis was visualized using the Click-iT protein synthesis assay kit (C10428, Life Technologies).

Isolation primary mouse pancreatic islets

Mouse islets were isolated by using collagenase and filtration as previously described (Johnson *et al.* 2003).

Tamoxifen administration

In this study, over a 5-day period, 4-week-old male mice were injected intraperitoneally with three doses of 2.5 mg tamoxifen (Sigma, T5648) freshly dissolved in corn oil at 10 mg/mL (Wicksteed *et al.* 2010).

http://joe.endocrinology-journals.org
https://doi.org/10.1530/JOE-18-0015

Autocrine effect of released insulin

To determine the influence of an autocrine effect of released insulin on cell death, we incubated MIN6 cells with 2.5 mM and 25 mM glucose serum-free DMEM. One day after Pdx1 knockdown (KD) in MIN6 cells, MIN6 cells were serum and glucose deprived for 24 h (DMEM, 2.5 mM glucose, no serum), and then maintained in culture in DMEM (no serum) supplemented with 2.5 or 25 mM glucose for 48 h. Then, the cell death was determined by propidium iodide (PI) staining.

In vivo characterization of mice

The *Pdx1*$^{+/-}$ mice have been previously described (Ren *et al.* 2014*a*). *Tsc1*$^{flox/flox}$ mice were purchased from the Jackson Laboratory and *MIP-Cre/ERT* (here referred to *Cre*) mice were provided by Louis Philipson (University of Chicago) (Wicksteed *et al.* 2010). Mice were maintained on the mixed genetic background (C57Bl/6 × 129Sv). Male mice were fed a high-fat diet (HFD) containing 42% fat (Harlan Laboratories Inc., Indianapolis, IN, USA) from 5 weeks of age (1 week after tamoxifen injection) and provided with water *ad libitum* as previously described (Ren *et al.* 2014*a*). Intraperitoneal glucose tolerance tests (GTTs) were performed on mice after a 5-h fast (2 g/kg dextrose) at age of 17 weeks (12 weeks for HFD). Insulin levels were measured after 5-h fasting and 10 min after glucose challenge. Insulin tolerance tests were performed after a 5-h fast by administering human recombinant insulin (0.75 U/kg). We quantified β-cell area from anti-insulin-stained pancreas sections counterstained with hematoxylin using the intensity thresholding function of the integrated morphometry package in ImageJ. BrdU (Sigma-Aldrich) was injected intraperitoneally (100 mg/kg) every 24 h, starting 3 days before killing, three injections in total (Stolovich-Rain *et al.* 2012). TUNEL labeling, Ki-67 staining, BrdU labeling and β-cell size measurement were performed as previously described (Chintinne *et al.* 2012, Ren *et al.* 2014*a*). For Ki67 staining and BrdU, at least 20,000 β-cells or 100 islets were counted. For TUNEL staining, more than 10,000 β-cells were counted. Only Ki67 or BrdU and insulin double-positive cells were counted as Ki67+ or BrdU+ β-cell in islets. All animal experiments in this study were performed under protocols approved by the University of Chicago Animal Studies Committee and were conducted in accordance with National Institutes of Health guidelines for the care and use of animals in research.

Rapamycin treatment studies

Rapamycin (Sigma) was initially dissolved in 100% ethanol, stored at −20°C and further diluted in an aqueous solution of 5.2% Tween-80 and 5.2% PEG 400 (final ethanol concentration 2%) immediately before use (Mori *et al.* 2009*b*). Four-week-old mice were injected with tamoxifen. After being on HFD for 4 weeks, these mice were injected with rapamycin intraperitoneally (1 mg/kg body weight every other day) for 4 weeks with HFD. The mice were fed HFD for 12 weeks.

Imaging studies of pancreatic islets

Formalin-fixed pancreas sections underwent antigen retrieval in boiling citrate buffer (pH 6.0) for 10 min before labeling with antibodies against insulin (A0564; Dako), glucagon (G2654; Sigma-Aldrich) and DAPI (P-36931; Invitrogen).

Statistical analysis

ANOVA was used to assess the statistical significance of differences. Differences were considered significant when $P<0.05$. In all experiments, the number of asterisks is used to designate the following levels of statistical significance: ***$P<0.001$, **$P<0.01$, *$P<0.05$ compared with control group or *WT* group. ####$P<0.001$, ##$P<0.01$, #$P<0.05$ compared with *Pdx1*$^{+/-}$*Tsc1*$^{F/F}$*Cre*$^{-}$ group. Results are presented as mean ± S.E.M. Each experiment was repeats at least three times.

Results

The expression levels of Tsc1 are increased in Pdx1-deficient β-cells

Our previous studies showed *Pdx1*$^{+/-}$ mice develop diabetes due to decreasing β-cell mass, which is related to β-cell death (Ren *et al.* 2014*b*). To investigate whether Pdx1 also affect β-cell proliferation, β-cell proliferation in islets from *WT* and *Pdx1*$^{+/-}$ mice was determined by Ki67 staining and BrdU labeling. Ki67+ and BrdU+ β-cells were significantly decreased in *Pdx1*$^{+/-}$ mice compared to *WT* mice ($P<0.001$ and $P<0.05$ respectively, Fig. 1A). These results indicate that Pdx1 deficiency in mice significantly decreases β-cell proliferation. The effects of Pdx1 on TSC-mTORC1 pathway in MIN6 cells were next determined since this pathway is known to play a major role in hormonal and

http://joe.endocrinology-journals.org
https://doi.org/10.1530/JOE-18-0015

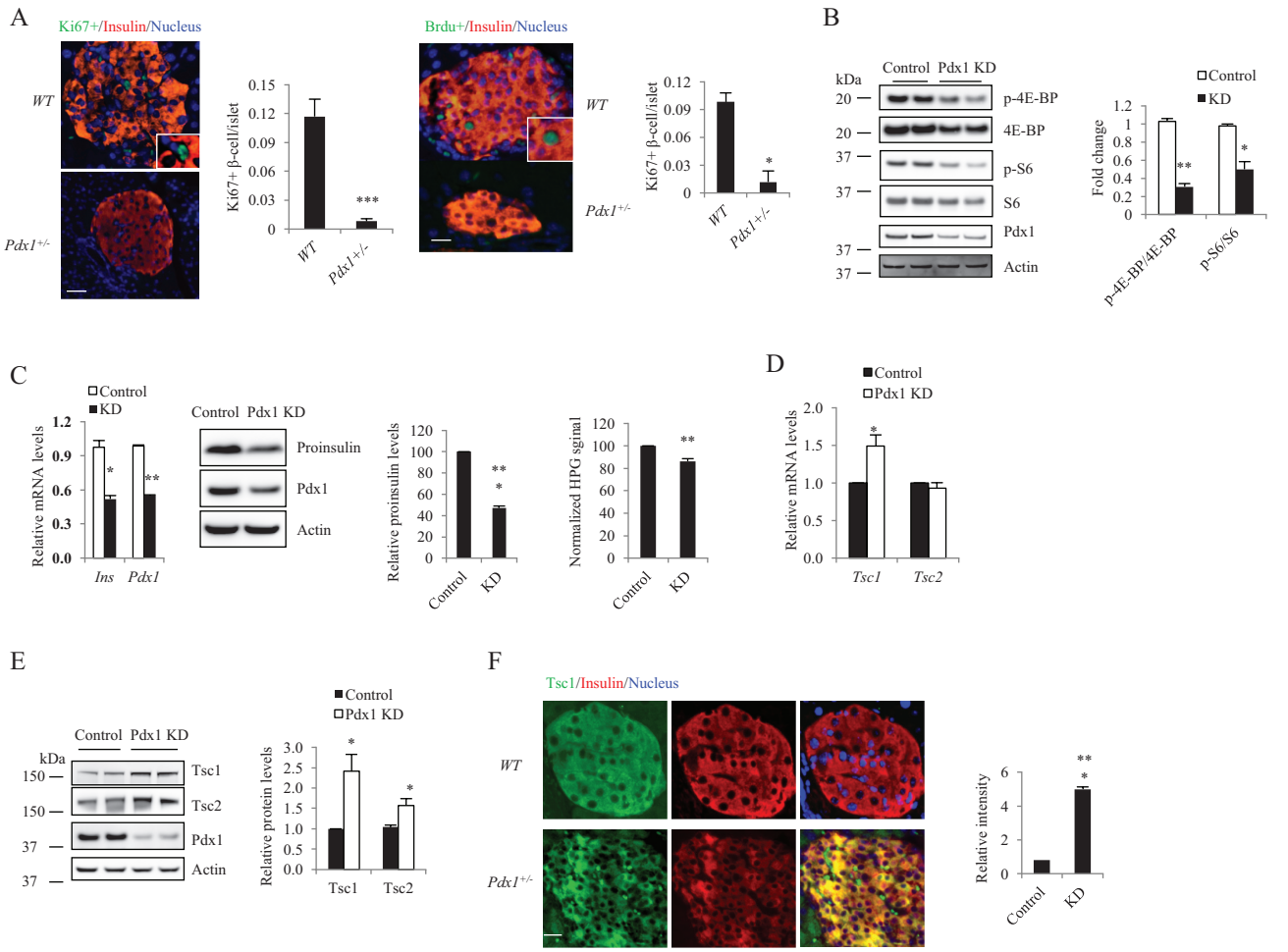

Figure 1

The expression levels of Tsc1 are increased in *Pdx1*$^{+/-}$ β-cells. (A) Ki67 staining and BrdU labeling of *Pdx1*$^{+/-}$ β-cells demonstrating a significant reduction in 15-week HFD-fed *Pdx1*$^{+/-}$ mice. ***$P<0.001$ compared to *WT*. (B) Pdx1 suppression inhibits mTORC1 activity. (C) Pdx1 suppression leads to an inhibition of insulin transcription and translation. (D) Pdx1 suppression induces an increase in mRNA (D) and protein levels of Tsc1 (E) in MIN6 cells. The mRNA levels of Tsc2 are not changed. Three days after Pdx1 shRNA lentivirus infection in MIN6 cells, mRNA and proteins levels were analyzed by QRT-PCR (C and D) and Western blot (B, C and E), respectively. *$P<0.05$ compared to control group. Nascent protein synthesis was detected by Click-iT protein synthesis assay kit according to the instruction. (F) Elevated Tsc1 expression in 20-week old *Pdx1*$^{+/-}$ islets. Immunofluorescence staining of the pancreatic sections from mice with 15-week HFD was performed with Tsc1 antibody. The scale bar represents 20 μm.

nutritional signals that regulate cell size and proliferation. Pdx1 was knocked down in MIN 6 cells using shRNA lentivirus. Indeed, Pdx1 suppression inhibited mTORC1 activity as shown by decreasing phosphorylation of 4E-BP and S6 (Fig. 1B), both molecules are downstream effectors of mTORC1. Phosphorylation of 4E-BP and S6 were decreased by 70% and 50%, respectively (Fig. 1B). Since a reduction in phosphorylation of S6 may suggest a reduced translational activity, we determined the effect of Pdx1 KD on insulin transcription and translation. Pdx1 KD in MIN6 cells induced a significant reduction of mRNA levels of insulin by 44.5% ($P<0.05$, Fig. 1C). The protein levels of proinsulin were decreased by 52.9% in Pdx1 KD MIN6 cells. These results indicate that Pdx1 deficiency also induces a reduction of insulin translation by 8%. In consistent with these results, Pdx1 KD in MIN6 cells significantly decreased nascent protein synthesis by 14% (Fig. 1C). As the TSC tumor suppressor complex (TSC1/TSC2) is a critical negative regulator of mTORC1, we studied the effect of Pdx1 suppression on expression levels of Tsc1 and Tsc2. The results showed that Pdx1 suppression induced an increase in Tsc1 mRNA levels by 49% ($P<0.05$, Fig. 1D). However, Pdx1 KD had no effect on Tsc2 mRNA levels (Fig. 1D). Interestingly, both Tsc1 and Tsc2 protein levels were increased in Pdx1 KD cells (Fig. 1E). Pdx1 suppression induced an increase in Tsc1 protein levels by 140% ($P<0.05$) and Tsc2 protein levels by 50% ($P<0.05$), respectively (Fig. 1E). IFC staining also

http://joe.endocrinology-journals.org
https://doi.org/10.1530/JOE-18-0015

clearly showed elevated TSC1 expression in *Pdx1*$^{+/-}$ islets (Fig. 1F). These results indicate that Pdx1 suppression elevates Tsc1 and Tsc2 expression.

Effect of Tsc1 ablation in adult Pdx1$^{+/-}$ mice

To investigate the function of the TSC-mTOR pathway in pancreatic β-cells, we established a mouse model with pancreatic β-cell-specific deletion of *Tsc1*. Mice containing homozygous floxed *Tsc1* alleles (*Tsc1*$^{F/F}$) were mated with the *Cre* transgenic line driven by the mouse *Ins1* promoter (*MIP-Cre/ERT*, here refers to *Cre*). Pancreatic islets from *Pdx1*$^{+/-}$*Tsc1*$^{F/F}$*Cre*$^{-}$ mice were small and contained reduced numbers of insulin-containing β-cells (Fig. 2A). Pancreatic islets from *Tsc1*$^{F/F}$*Cre*$^{+}$ mice appeared bigger than those from *Tsc1*$^{F/F}$*Cre*$^{-}$ mice (Fig. 2A). β-cells in *Pdx1*$^{+/-}$*Tsc1*$^{F/F}$*Cre*$^{-}$ islets also exhibited increased TUNEL labeling ($P<0.05$) (Fig. 2B). However, this parameter was not significantly decreased in *Tsc1*$^{F/F}$*Cre*$^{+}$ and Pdx1$^{+/-}$*Tsc1*$^{F/F}$*Cre*$^{+}$ mice compared to *Tsc1*$^{F/F}$*Cre*$^{-}$ or *Pdx1*$^{+/-}$*Tsc1*$^{F/F}$*Cre*$^{-}$, respectively (Fig. 2B). To determine whether *Tsc1* ablation affects β-cell proliferation, islets were stained for the proliferative marker Ki-67. Compared to *Tsc1*$^{F/F}$*Cre*$^{-}$, β-cell proliferation was decreased in *Pdx1*$^{+/-}$*Tsc1*$^{F/F}$*Cre*$^{-}$ islets ($P<0.001$) and was significantly improved by *Tsc1* ablation in *Pdx1*$^{+/-}$*Tsc1*$^{F/F}$*Cre*$^{+}$ islets ($P<0.05$, Fig. 2C). The *Tsc1*$^{F/F}$*Cre*$^{+}$ mice showed an increase in β-cell mass by 138% compared to that in *Tsc1*$^{F/F}$*Cre*$^{-}$ mice ($P<0.001$, Fig. 2D). β-cell mass in *Pdx1*$^{+/-}$*Tsc1*$^{F/F}$*Cre*$^{+}$ mice was restored to the value in *Tsc1*$^{F/F}$*Cre*$^{-}$ mice and β-cell mass approximately doubled compared to *Pdx1*$^{+/-}$*Tsc1*$^{F/F}$*Cre*$^{-}$ mice ($P<0.05$) (Fig. 2D). Given enlargement of islets observed in the p-S6 staining and to determine whether the increase in islet mass reflected increased cell size in addition to cell proliferation, we also measured the size of individual β-cells. We found that β-cells in *Tsc1*$^{F/F}$*Cre*$^{+}$ islets were significantly larger than those in *Tsc1*$^{F/F}$*Cre*$^{-}$ islets. β-cell size increased by 87% ($P<0.05$). β-cell size increased by 73% in *Pdx1*$^{+/-}$*Tsc1*$^{F/F}$*Cre*$^{+}$ islets compared to *Pdx1*$^{+/-}$*Tsc1*$^{F/F}$*Cre*$^{-}$ islets ($P<0.05$, Fig. 2E). In contrast, although β-cell size was smaller in *Pdx1*$^{+/-}$*Tsc1*$^{F/F}$*Cre*$^{-}$ islets, we did not observe significant differences in β-cell size between *Tsc1*$^{F/F}$*Cre*$^{-}$ and *Pdx1*$^{+/-}$*Tsc1*$^{F/F}$*Cre*$^{-}$ islets. These results indicate that *Tsc1* ablation in β-cells decreases β-cell apoptosis, increases β-cell proliferation, β-cell size and β-cell mass.

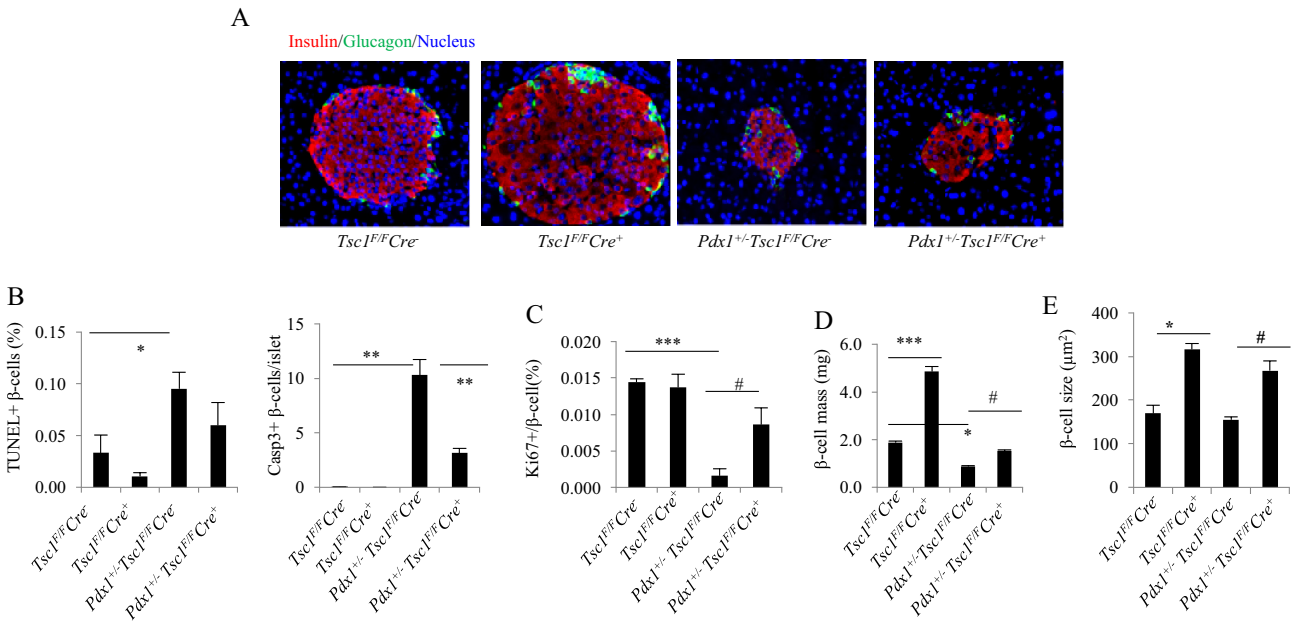

Figure 2
Tsc1 ablation preserves β-cells mass in adult *Pdx1*$^{+/-}$ mice. (A) Islet morphology in adult mice on a HFD for 12 weeks; anti-insulin and anti-glucagon antibodies were used to stain β-cells (red) and α cells (green), respectively. The scale bar represents 20 μm. (B and C) TUNEL, cleaved caspase3 staining and Ki67^{+} labeling of pancreatic β-cells in 12-week HFD-fed mice. Quantitative TUNEL, cleaved caspase3 (B) and Ki67+ β-cells (C) data are shown. *$P<0.05$ and ***$P<0.001$ compared to the *Tsc1*$^{F/F}$*Cre*$^{-}$ mice ($n=3$-5 per group). #$P<0.05$ compared to *Pdx1*$^{+/-}$ *Tsc1*$^{F/F}$*Cre*$^{-}$ mice. (D) Histological analysis of pancreatic islets in 12-week HFD-fed mice and quantitation of group data for β-cells mass are shown ($n=3$-5 per group). *$P<0.05$, **$P<0.01$ compared to the *Tsc1*$^{F/F}$*Cre*$^{-}$ mice. #$P<0.05$ compared to *Pdx1*$^{+/-}$ *Tsc1*$^{F/F}$*Cre*$^{-}$ mice. (E) β-cell size increases in 12-week HFD-fed mice *Pdx1*$^{+/-}$*Tsc1*$^{F/F}$*Cre*$^{+}$ mice. Pancreatic sections were stained with anti-insulin antibody to determine the size of individual β-cells. The data showed an average size of ≥2000 β-cells from each of three mice of each genotype. *$P<0.05$ compared to *Tsc1*$^{F/F}$*Cre*$^{-}$ mice and #$P<0.05$ compared to *Pdx1*$^{+/-}$ *Tsc1*$^{F/F}$*Cre*$^{-}$ mice. Values are mean ± S.E.M.

http://joe.endocrinology-journals.org
https://doi.org/10.1530/JOE-18-0015

Tsc1 gene ablation prevents diabetes in Pdx1$^{+/-}$ mice

To rule out the effect of *Cre* itself on mice, we first determined the effect of *Cre* on the *Pdx1*$^{+/-}$ mice. We performed GTTs on these mice with HFD. The results showed that both *Pdx1*$^{+/-}$*Cre*$^{-}$ and *Pdx1*$^{+/-}$*Cre*$^{+}$ mice showed glucose intolerance and had a similar response to glucose (Supplementary Fig. 1, see section on supplementary data given at the end of this article). In addition, compared to *Cre*$^{+}$ mice, *Pdx1*$^{+/-}$*Cre*$^{+}$ mice significantly increased blood glucose levels ($P<0.01$ and $P<0.001$) (Supplementary Fig. 1). Thus, *MIP-Cre/ER* transgene itself is not affecting β-cell function in response to glucose. To determine whether enhanced β-cell size and proliferation due to *Tsc1* ablation prevents the diabetic phenotype in *Pdx1*$^{+/-}$ mice, we performed GTT and insulin tolerance tests (ITTs) on *Pdx1*$^{+/-}$*Tsc1*$^{F/F}$*Cre*$^{-}$, *Pdx1*$^{+/-}$*Tsc1*$^{F/F}$*Cre*$^{+}$ mice. Male *Pdx1*$^{+/-}$*Tsc1*$^{F/F}$*Cre*$^{-}$ mice on HFD develop increased fasting blood glucose and impaired glucose clearance (Fig. 3A and B). Fasting blood glucose levels were increased in Pdx1$^{+/-}$*Tsc1*$^{F/F}$*Cre*$^{-}$ mice compared to *Tsc1*$^{F/F}$*Cre*$^{-}$ mice on HFD for 11 weeks ($P<0.001$) (Fig. 3A). However, *Pdx1*$^{+/-}$*Tsc1*$^{F/F}$*Cre*$^{+}$ mice exhibited significantly lower fasting blood glucose (Fig. 3A and B). The blood glucose in *Pdx1*$^{+/-}$*Tsc1*$^{F/F}$*Cre*$^{+}$ mice was decreased by 34% compared with that in *Pdx1*$^{+/-}$*Tsc1*$^{F/F}$*Cre*$^{-}$ mice (Fig. 3A). The *Pdx1*$^{+/-}$*Tsc1*$^{F/F}$*Cre*$^{+}$ mice demonstrated improved glucose tolerance and had normal glucose tolerance compared to *Tsc1*$^{F/F}$*Cre*$^{-}$ mice, indicating that *Tsc1* ablation prevents diabetes in *Pdx1*$^{+/-}$*Tsc1*$^{F/F}$*Cre*$^{-}$ mice (Fig. 3B). The area under the blood glucose curve (AUC) decreased by 51% in *Pdx1*$^{+/-}$*Tsc1*$^{F/F}$*Cre*$^{+}$ mice compared to *Pdx1*$^{+/-}$*Tsc1*$^{F/F}$*Cre*$^{-}$ mice ($P<0.001$) (Fig. 3C). The response to exogenous insulin was significantly increased in *Pdx1*$^{+/-}$*Tsc1*$^{F/F}$*Cre*$^{+}$ and *Tsc1*$^{F/F}$*Cre*$^{+}$ mice compared to *Pdx1*$^{+/-}$*Tsc1*$^{F/F}$*Cre*$^{-}$ and *Tsc1*$^{F/F}$*Cre*$^{-}$ (both $P<0.05$), respectively. The reduction in blood glucose in *Pdx1*$^{+/-}$*Tsc1*$^{F/F}$*Cre*$^{+}$ mice after insulin administration was similar to *Tsc1*$^{F/F}$*Cre*$^{+}$ mice (Fig. 3D). At 14 weeks on HFD, fasting insulin levels in *Pdx1*$^{+/-}$*Tsc1*$^{F/F}$*Cre*$^{-}$ mice were 45% of the values in *Tsc1*$^{F/F}$*Cre*$^{-}$ animals (Fig. 3E), and these levels were increased in *Pdx1*$^{+/-}$*Tsc1*$^{F/F}$*Cre*$^{+}$ mice both under basal conditions ($P<0.001$) and following glucose challenge ($P<0.001$) (Fig. 3E). There were no significant differences in body weight in the four groups of mice (Supplementary Fig. 2). Together with the above results, we conclude that *Tsc1* ablation in β-cells prevents the diabetic phenotype in the *Pdx1*$^{+/-}$*Tsc1*$^{F/F}$*Cre*$^{-}$ mouse by reducing apoptotic β-cell death, increasing β-cell proliferation, preserving glucose tolerance and increasing the response to exogenous insulin.

β-cell-specific Tsc1 deletion activates mTORC1 in islets

Tsc1 mRNA levels were assayed in islets by QRT-PCR after tamoxifen treatment. Tamoxifen treatment significantly reduced Tsc1 mRNA levels by 68% and 65% in islets from *Tsc1*$^{F/F}$*Cre*$^{+}$ mice on normal chow ($P<0.001$,

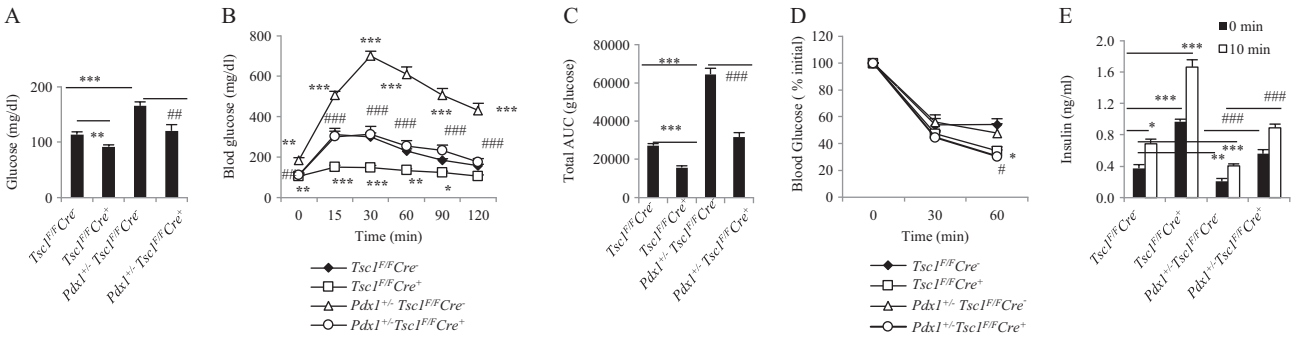

Figure 3
Tsc1 gene ablation prevents diabetes in *Pdx1*$^{+/-}$ mice. (A) Overnight fasting glucose levels were measured in male mice on HFD for 13 weeks ($n=8$–12). ***$P<0.001$ compared to the *Tsc1*$^{F/F}$*Cre*$^{-}$ mice. ###$P<0.01$ compared to *Pdx1*$^{+/-}$*Tsc1*$^{F/F}$*Cre*$^{-}$ mice. (B) Blood glucose levels after intraperitoneal injection of dextrose (1 g/kg) in the male mice at 13 weeks with HFD. *$P<0.05$, **$P<0.01$, ***$P<0.001$ compared to the *Tsc1*$^{F/F}$*Cre*$^{-}$ mice. ##$P<0.01$, ###$P<0.001$ compared to *Pdx1*$^{+/-}$*Tsc1*$^{F/F}$*Cre*$^{-}$ mice ($n=8$–22). (C) Area under the blood glucose curves (AUC) using the data from B in the four mouse groups designated. ***$P<0.001$ compared to the *Tsc1*$^{F/F}$*Cre*$^{-}$ mice. ###$P<0.001$ compared to *Pdx1*$^{+/-}$*Tsc1*$^{F/F}$*Cre*$^{-}$ mice. (D) Glucose levels in response to 0.75 U/kg body weight insulin in the four male mouse groups designated at 14 weeks with HFD ($n=12$-22). *$P<0.05$, *Tsc1*$^{F/F}$*Cre*$^{+}$ mice compared to *Tsc1*$^{F/F}$*Cre*$^{-}$ mice; #$P<0.05$, *Pdx1*$^{+/-}$*Tsc1*$^{F/F}$*Cre*$^{+}$ compared to *Pdx1*$^{+/-}$*Tsc1*$^{F/F}$*Cre*$^{-}$ mice. (E) Insulin levels measured fasting and 10 min after intraperitoneal dextrose in mice at 14 weeks with HFD. *$P<0.05$, **$P<0.01$, ***$P<0.001$ compared to the *Tsc1*$^{F/F}$*Cre*$^{-}$ mice. ###$P<0.001$ compared to *Pdx1*$^{+/-}$*Tsc1*$^{F/F}$*Cre*$^{-}$ mice. Values are mean ± S.E.M.

http://joe.endocrinology-journals.org
https://doi.org/10.1530/JOE-18-0015

Supplementary Fig. 3A) and HFD ($P<0.001$, Fig. 4A), respectively. To determine the molecular mechanism by which Tsc1 deletion in β-cells prevents diabetes induced by Pdx1 deficiency, activation of mTORC1 was measured. We determined the activation status of mTORC1 in islets by immunoblotting for S6 and 4E-BP phosphorylation (p-S6 and p-4E-BP), which serve as two convenient downstream readouts for mTORC1. Loss of Tsc1 was associated with increased p-S6 and p-4E-BP in *Tsc1$^{F/F}$Cre^{+}* islets (Supplementary Fig. 3B), indicating that mTORC1 was activated in the mutant islets. p-4E-BP and p-S6 were increased by 31% and 23-fold, respectively, in islets from *Tsc1$^{F/F}$Cre^{+}* mice compared to those in islets from *Tsc1$^{F/F}$Cre^{-}* mice ($P<0.001$) (Supplementary Fig. 3C). The data indicate that deletion of TSC1 from mice on a normal chow induce activation of mTORC1. Next, we determined whether loss of Tsc1 in Pdx1-deficient mice on HFD can prevent diabetes due to activation of mTORC1 in β-cells. Due to increasing β-cell death and decreasing β-cell size and proliferation, we could not isolate sufficient numbers of islets from *Pdx1$^{+/-}$Tsc1$^{F/F}$Cre^{-}* mice on HFD for immunoblotting. However, both p-4E-BP and p-S6 were significantly increased in islets from *Pdx1$^{+/-}$Tsc1$^{F/F}$Cre^{+}* mice (Fig. 4B). Interestingly, p-S6 from *Pdx1$^{+/-}$Tsc1$^{F/F}$Cre^{+}* islets was increased by more than 40-fold compared to that from *Tsc1$^{F/F}$Cre^{-}* islets, which was an even greater elevation than observed in *Tsc1$^{F/F}$Cre^{+}* islets (Fig. 4C).

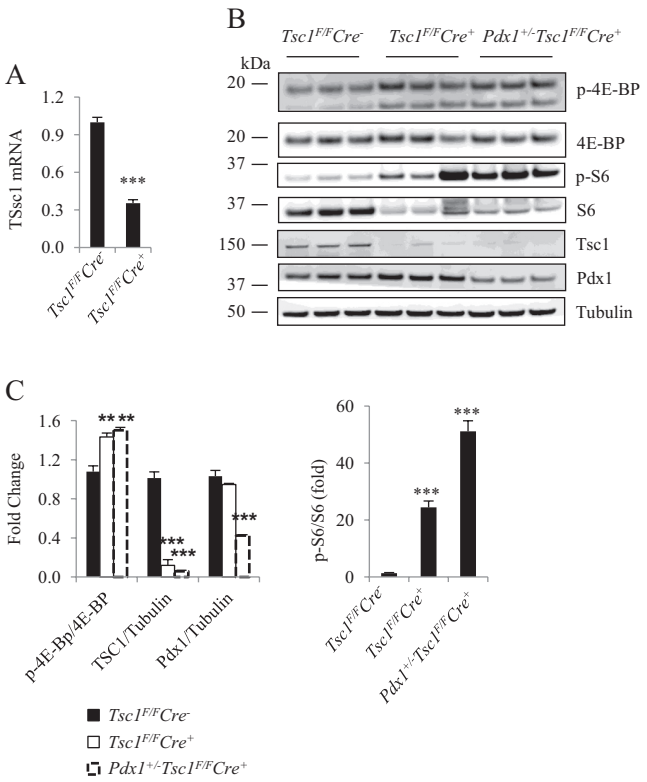

Figure 4
β-cell-specific Tsc1 deletion activates mammalian target of rapamycin (mTOR) complex 1 in islets. (A) Tsc1 mRNA levels were measured by QRT-PCR in islets from mice on HFD for 13 weeks. ***$P<0.001$ compared to control group. (B) Elevated 4E-BP and S6 phosphorylation in *Pdx1$^{+/-}$Tsc1$^{F/F}$cre^{+}* islets. Immunoblot analysis of phospho-4E-BP (p-4E-BP), 4E-BP, phospho-S6 (Ser$^{240/244}$, p-S6), S6, Tsc1 and Tubulin are shown. Islets were isolated from independent male mice on HFD for 15 weeks. (C) Bar graphs represent quantification using densitometry of the relative amounts of the indicated proteins determined by Western blots in D. ***$P<0.001$ compared to the *Tsc1$^{F/F}$Cre^{-}* mice.

To further determine whether *Tsc1* ablation in β-cells induces elevated S6 phosphorylation, S6 phosphorylation was determined in β-cells from *Tsc1$^{F/F}$Cre^{+}* and *Pdx1$^{+/-}$Tsc1$^{F/F}$Cre^{+}* mice by IFC and IHC methods. First, we determine the specificity of p-S6 antibody. The results showed that p-S6 was increased in islets from *Tsc1$^{F/F}$Cre^{+}* mice. However, p-S6 antibody-specific blocking peptide prevented pS6 antibody from recognizing the p-S6 in *Tsc1$^{F/F}$Cre^{+}* islets (Fig. 5A). These results indicate that P-S6 antibody is specific to detect phosphorylation of S6 in islets. Immunostaining for p-S6 within the pancreas showed that mTORC1 was activated only in the β-cells from *Tsc1$^{F/F}$Cre^{+}* and *Pdx1$^{+/-}$Tsc1$^{F/F}$Cre^{+}* mice not in the β-cells from *Tsc1$^{F/F}$Cre^{-}* and *Pdx1$^{+/-}$Tsc1$^{F/F}$Cre^{-}* mice and not the neighboring cells (Fig. 5B and C), which is consistent with the cell-autonomous effect of Tsc1 on mTORC1. These data also revealed large islets, suggesting the expansion of islet mass in the *Tsc1$^{F/F}$Cre^{+}* and *Pdx1$^{+/-}$Tsc1$^{F/F}$Cre^{+}* mice.

Rapamycin decreased mTORC1 activity in β-cells from Tsc1$^{F/F}$Cre^{+} and Pdx1$^{+/-}$Tsc1$^{F/F}$Cre^{+} mice

To further test the effects of mTORC1 activation on pancreatic β-cells, we treated 8-week-old mutant and control mice with vehicle and rapamycin, a specific mTORC1 inhibitor, at 1 mg/kg every other day for 4 weeks. The vehicle itself has no effect on the mice (Supplementary Fig. 4). The response of the mice after vehicle treatment to glucose and insulin is similar to Fig. 3B. However, after rapamycin treatment, fasting and feeding glucose levels were not significantly different between *Tsc1$^{F/F}$Cre^{-}* and *Tsc1$^{F/F}$Cre^{+}* mice (Fig. 6A and B). Rapamycin treatment significantly increased glucose levels in *Pdx1$^{+/-}$Tsc1$^{F/F}$Cre^{+}* mice compared to vehicle treatment (Supplementary Fig. 4). After rapamycin treatment, *Pdx1$^{+/-}$Tsc1$^{F/F}$Cre^{+}* mice showed similar feeding and fasting glucose levels compared to *Pdx1$^{+/-}$Tsc1$^{F/F}$Cre^{-}* (Fig. 6A and B). However, rapamycin-treated *Pdx1$^{+/-}$Tsc1$^{F/F}$Cre^{-}* mice showed

http://joe.endocrinology-journals.org
https://doi.org/10.1530/JOE-18-0015

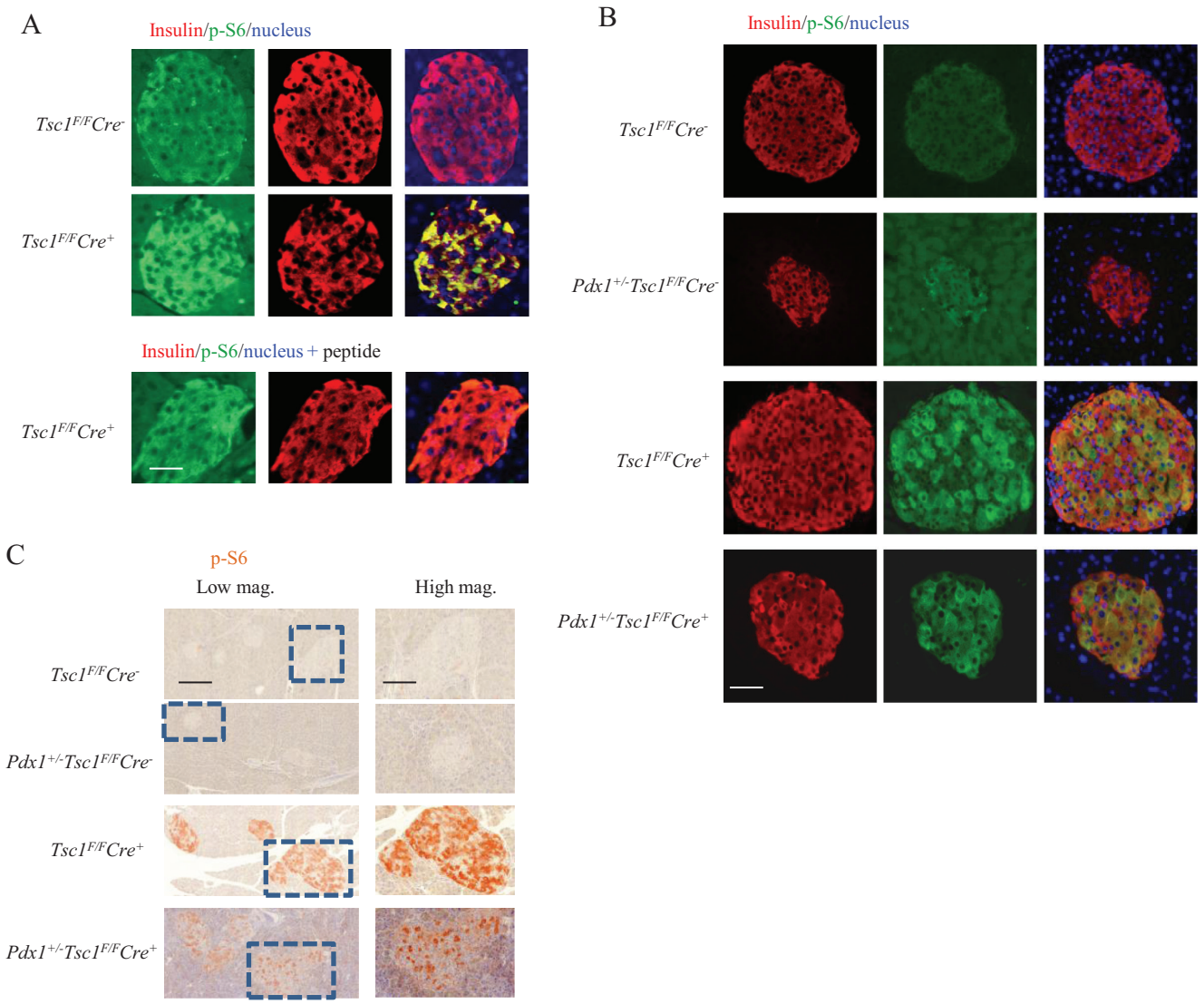

Figure 5
Elevated S6 phosphorylation in *Tsc1*$^{F/F}$*Cre*$^{+}$ and *Pdx1*$^{+/-}$*Tsc1*$^{F/F}$*Cre*$^{+}$ islets. (A) Specificity of p-S6 (Ser$^{235/236}$) antibody. For immunohistochemistry, 2 µL peptide was added to 1 µL antibody used in 100 µL total volume. The mixture was incubated for 30 min prior to adding the entire volume to the slide. Double labeling of the pancreatic sections from mice on HFD for 15 weeks was performed with p-S6 (Ser$^{235/236}$) antibody and insulin antibody. The scale bar represents 100 µm. (B) S6 phosphorylation was quantified in β-cells from *Tsc1*$^{F/F}$*Cre*$^{+}$ and *Pdx1*$^{+/-}$*Tsc1*$^{F/F}$*Cre*$^{+}$ mice. Double labeling of the pancreatic sections from mice on HFD for 15 weeks was performed with p-S6 (Ser$^{235/236}$) antibody and insulin antibody. The scale bar represents 100 µm. (C) Elevated S6 phosphorylation in *Tsc1*$^{F/F}$*Cre*$^{+}$ and *Pdx1*$^{+/-}$*Tsc1*$^{F/F}$*Cre*$^{+}$ islets. Immunostaining of the pancreatic sections from mice on HFD for 15 weeks was performed with p-S6 (Ser$^{235/236}$) antibody. The scale bar represents 200 µm (low mag., low magnification) and 100 µm (high mag., high magnification).

impaired glucose tolerance compared to *Pdx1*$^{+/-}$*Tsc1*$^{F/F}$*Cre*$^{+}$ mice (Fig. 6C). Indeed, after rapamycin treatment, the AUC was significantly higher in *Pdx1*$^{+/-}$*Tsc1*$^{F/F}$*Cre*$^{+}$ mice than in *Pdx1*$^{+/-}$*Tsc1*$^{F/F}$*Cre*$^{-}$ mice ($P<0.05$) (Fig. 6D), while the *Tsc1*$^{F/F}$*Cre*$^{-}$ and *Tsc1*$^{F/F}$*Cre*$^{+}$ mice showed similar AUC ($P>0.05$) (Fig. 6D). Indeed, rapamycin treatment inhibited the increase in phosphorylation of S6 in *Tsc1*$^{F/F}$*Cre*$^{+}$ and *Pdx1*$^{+/-}$*Tsc1*$^{F/F}$*Cre*$^{+}$ islets (Fig. 6E). Thus, rapamycin treatment abrogated the increased mTORC1 activity in the mutant pancreatic β-cells. The effects of treating mutant animals with rapamycin were attributable to the inhibition of the increase of mTORC1 activity in β-cells.

Pdx1 suppression decreases AKT activity

To determine the mechanism by which Pdx1 suppression decreases mTORC1, we knocked down Pdx1 in MIN6 cells. Since both AKT and GSK3β are involved in regulating

http://joe.endocrinology-journals.org
https://doi.org/10.1530/JOE-18-0015

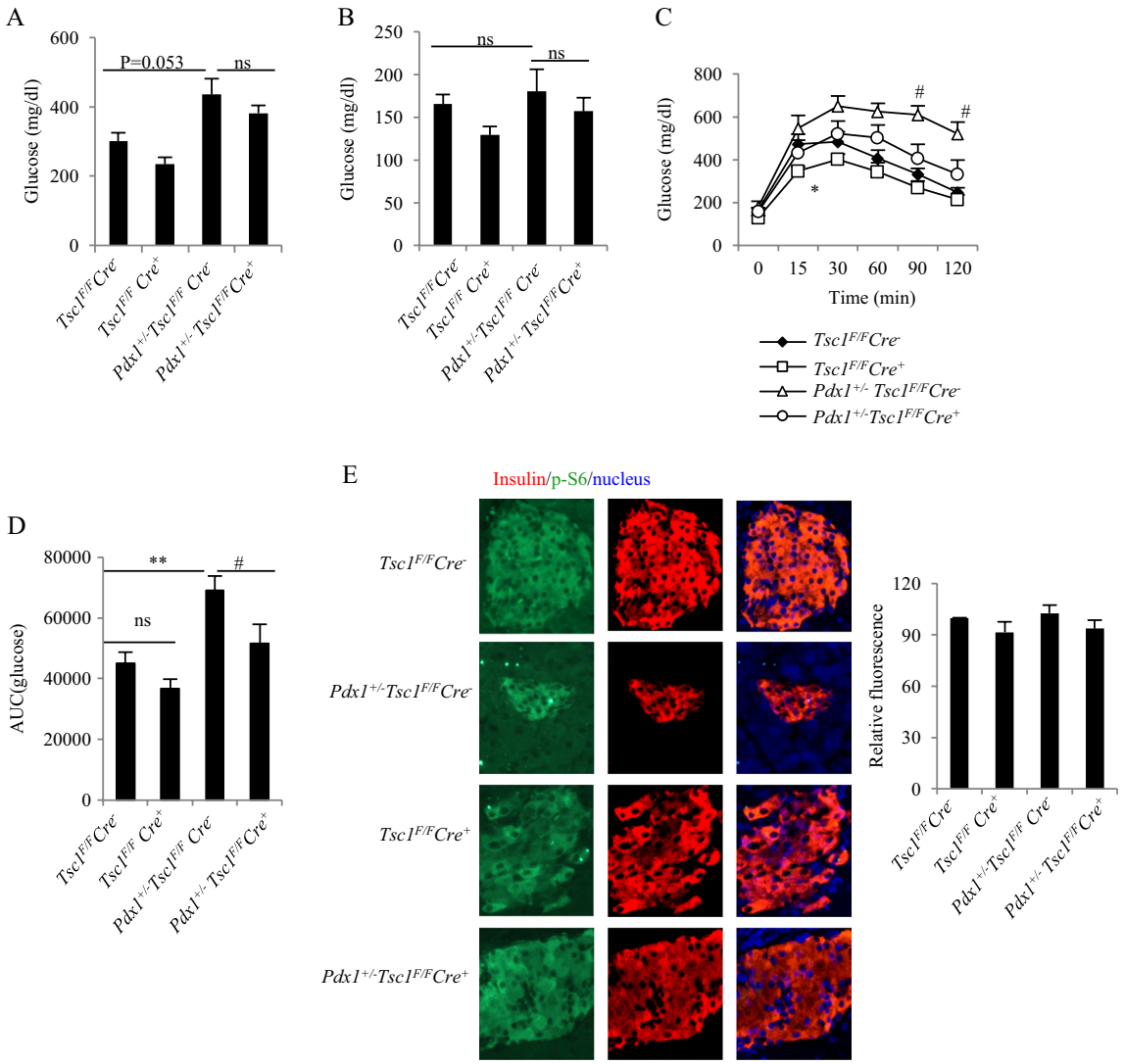

Figure 6

Rapamycin decreased mTORC1 activity in β-cells from *Tsc1*$^{F/F}$*Cre*$^{+}$ and *Pdx1*$^{+/-}$*Tsc1*$^{F/F}$*Cre*$^{+}$ mice. (A) Glucose levels after feeding. (B) Glucose levels after fasting. The glucose levels were measured in male mice with rapamycin treatment on HFD for 11 weeks (A) and 12 weeks (B) (n=8–10). ns, not significant. (C) Blood glucose levels after intraperitoneal injection of dextrose (1 g/kg) in the male mice with rapamycin treatment on HFD for 12 weeks. *P<0.05 compared to the *Tsc1*$^{F/F}$*Cre*$^{-}$ mice (n=8-9). (D) Area under the blood glucose curves (AUC) using the data from C in the four mouse groups designated. ns, not significant. (E) Rapamycin treatment inhibits S6 phosphorylation. Double labeling of the pancreatic sections from mice on HFD for 15 weeks was performed with p-S6 (Ser$^{235/236}$) antibody and insulin antibody. The scale bar represents 100 μm. Values are mean ± S.E.M.

mTORC1 activity, the phosphorylation of AKT and GSK3β were determined. The results showed that IGF-1 rapidly stimulated Akt phosphorylation in control cells by 4.7-fold, but Pdx1 KD significantly decreased IGF-1-induced Akt phosphorylation by 68% (Fig. 7A). To determine the possibility of an autocrine effect of released insulin, the cell death was determined in Pdx1 KD MIN6 cells. The results showed that Pdx1 KD induced a significant increase in cell death in MIN6 cells with 2.5 mM glucose (Fig. 7B). The increasing glucose concentrations resulted in inhibition of cell death around by 10% (Fig. 7B). The results indicate that the autocrine released insulin due to higher glucose increases cell survival. Pdx1 KD also significantly decreased insulin release and content (Fig. 7C). In addition, Pdx1 KD induced a decrease in GSK3β protein levels, whereas phosphorylation of GSK3β at Ser9 was not significantly different from the control cells (Fig. 7D). The model of Pdx1 in regulating Tsc-mTORC1 pathway is shown in Fig. 7E. Pdx1 suppression decreases AKT activity, and increases Tsc1 and Tsc2, leading to the decrease in mTORC1-mediated β-cell size and proliferation.

http://joe.endocrinology-journals.org
https://doi.org/10.1530/JOE-18-0015

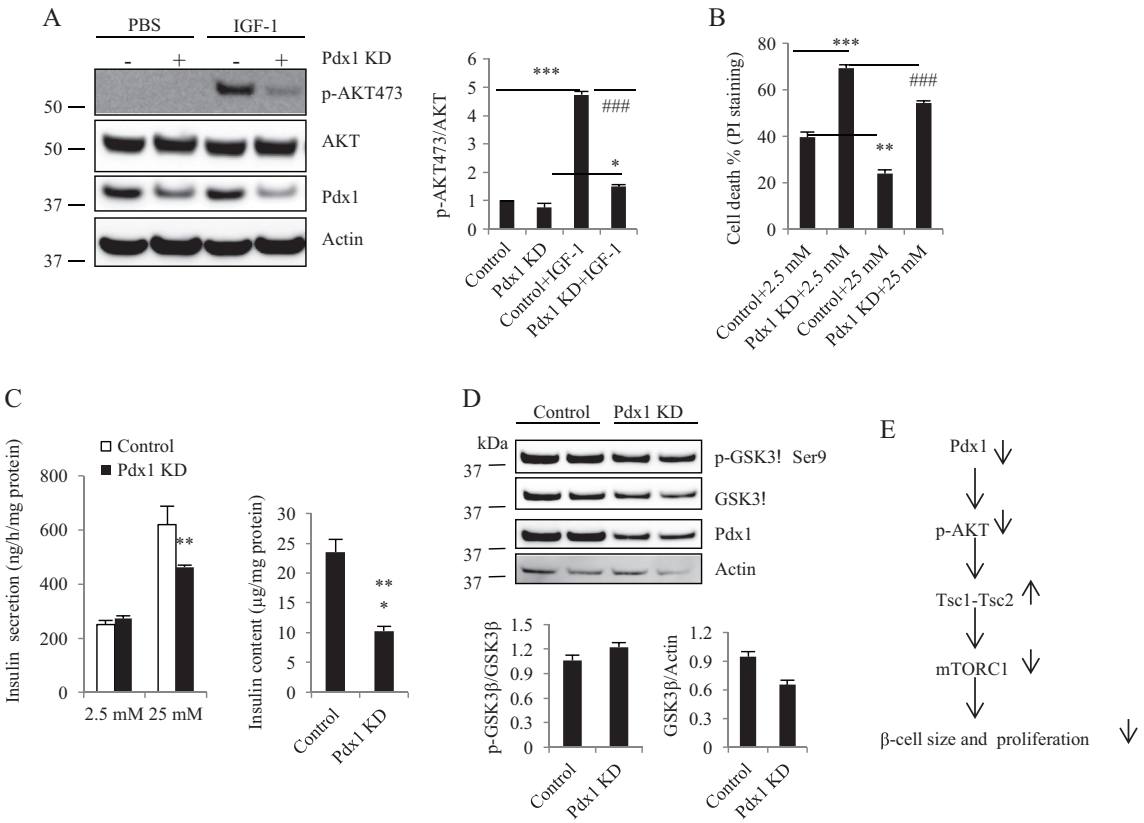

Figure 7

Pdx1 suppression decrease AKT activity in MIN6 cells. (A) Pdx1 KD inhibits IGF-I-stimulated Akt activation in MIN6 cells. Three days after Pdx1 shRNA lentivirus infection in MIN6 cells, MIN6 cells were deprived of serum for 16 h. Cells were stimulated with IGF-1 (100 ng/mL) for 10 min prior to lysis. p-Akt and Akt were assessed by Western immunoblotting. One representative blot is shown. Graphs display densitometry measurements of relative levels and represent means ± S.E. of two independent experiments. *$P<0.05$, ***$P<0.001$, ###$P<0.001$. (B) The effect of an autocrine effect of released insulin on cell death. One day after Pdx1 KD in MIN6 cells, MIN6 cells were serum and glucose deprived for 24 h (DMEM, 2.5 mM glucose, no serum) then maintained in culture in DMEM (no serum) supplemented with 2.5 or 25 mM glucose for 48 h. Then, the cell death was determined by PI staining. **$P<0.01$, ***$P<0.001$, ###$P<0.01$. (C) Insulin secretion and content in Pdx1 KD MIN6 cells. Three days after culture with control or Pdx1 shRNA lentivirus, MIN6 cells were washed twice in DMEM without serum and glucose, and then were pre-incubated with 2.5 mM glucose for 1h prior to switching to 2.5 or 25 mM glucose for 1 h at 37°C. Insulin concentration in the medium and insulin content were measured by ELISA assay. (D) Three days after Pdx1 shRNA lentivirus infection in MIN6 cells, the proteins levels of Pdx1, p-GSK3β and GSK3β were determined by Western blot. Bar graphs represent quantification using densitometry of the relative amounts of the indicated proteins determined by Western Blots. (E) Model of Pdx1 in regulating Tsc1-mTORC1 pathway. Pdx1 suppression increases Tsc1 and Tsc2 and decreases AKT activity, leading to the decrease in mTORC1-mediated β-cell size and proliferation.

Discussion

Our studies have demonstrated that Pdx1-deficient mice develop hyperglycemia associated with an increase in β-cell death and a decrease in β-cell mass (Ren *et al.* 2014*a*). The present studies were undertaken to further define the molecular mechanisms responsible for the reduction in pancreatic β-cell mass induced by Pdx1 deficiency. The *Pdx1*$^{+/-}$ mice showed decreased β-cell mass associated with a failure of β-cell size and proliferation. To examine the role of mTOR in β-cell size and proliferation in Pdx1-deficient mice, we generated β-cell-specific *Tsc1* KO mice, in which *MIP-Cre/ER* deletes the *Tsc1* gene only in pancreatic β-cells and studied β-cell function in these animals. Although *MIP-Cre/ER* mice are known to possess abnormal β-cell size characteristics related to expression of the hGH minigene (Oropeza *et al.* 2015), the response of *Pdx1*$^{+/-}$*Cre*$^{+}$ to glucose in this study was not different compared to Pdx1$^{+/-}$Cre^{-}, indicating that *MIP-Cre/ER* itself has minimal effect on mice. As expected, *Tsc1*$^{F/F}$*Cre*$^{+}$ mice manifested increased islet mass, β-cell size and insulin secretion. Our results are consistent with other studies (Rachdi *et al.* 2008, Shigeyama *et al.* 2008, Liu *et al.* 2009, Mori *et al.* 2009*b*, Wittenberg *et al.* 2016). Although β-cell proliferation was not significantly increased in *Tsc1*$^{F/F}$*Cre*$^{+}$ mice compared to *Tsc1*$^{F/F}$*Cre*$^{-}$, *Pdx1*$^{+/-}$*Tsc1*$^{F/F}$*Cre*$^{+}$ mice showed an increase in β-cell proliferation, which may be caused by inactivation of 4E-BP. Moreover, *Pdx1*$^{+/-}$*Tsc1*$^{F/F}$*Cre*$^{+}$ mice showed an increase in β-cell size. Both increased β-cell size and proliferation may contribute to increased

http://joe.endocrinology-journals.org
https://doi.org/10.1530/JOE-18-0015

β-cell mass in *Pdx1*$^{+/-}$*Tsc1*$^{F/F}$*Cre*$^{+}$ mice. Based on the data in Fig. 2D, β-cell mass is increased by 75% in *Pdx1*$^{+/-}$*Tsc1*$^{F/F}$*Cre*$^{+}$ mice than that in *Pdx1*$^{+/-}$*Tsc1*$^{F/F}$*Cre*$^{-}$ mice. β-cell size is increased by 70% in *Pdx1*$^{+/-}$*Tsc1*$^{F/F}$*Cre*$^{+}$ mice compared to *Pdx1*$^{+/-}$*Tsc1*$^{F/F}$*Cre*$^{-}$ mice. Therefore, the increase in β-cell size is the main cause of the almost complete recovery of β-cell mass by mTORC1 activation in Pdx1 deficiency in HFD feeding. In addition, the protein levels of p-S6 in *Pdx1*$^{+/-}$*Tsc1*$^{F/F}$*Cre*$^{+}$ mouse islets are highly increased. It suggests that S6K activity is highly increased in these islets. Excessive and constant S6K activity leads to IRS2 downregulation that impairs survival and proliferation of β-cells (Shah *et al.* 2004). It is possible that remarkable increase in p-S6 in *Pdx1*$^{+/-}$*Tsc1*$^{F/F}$*Cre*$^{+}$ mouse islets might impair the full recovery of β-cell proliferation and survival. Fasting hypoglycemia and deletion of Tsc1 in Pdx1-deficient mice increased plasma insulin to the levels of *WT* mice but not to the levels of *Tsc1*$^{F/F}$*Cre*$^{+}$ mice, which indicates that Tsc1 inhibition counteracted the Pdx1 deficiency to some extent, but there is still a remaining effect, which is not abrogated by Tsc1 deletion. The result also suggests that the regulation of insulin gene by Pdx1 may be Tsc1 independent. Moreover, rapamycin treatment has been shown to have mixed effects on β-cells, depending on the experimental conditions (28). Rapamycin treatment can cause reductions in β-cell size, mass, proliferation and insulin secretion alongside increases in apoptosis (28). In this study, rapamycin treatment reversed the improved glucose tolerance observed in *Pdx1*$^{+/-}$*Tsc1*$^{F/F}$*Cre*$^{+}$ mice, while glucose tolerance was higher in all the Pdx1-deficient mice. Such results may be due to β-cell toxicity induced by rapamycin treatment and rapamycin may induce apoptosis in Pdx1-deficient β-cells. However, the mechanisms involved in inhibition of the TORC1 complex by rapamycin are complex. The individual contribution of 4EBP or S6K to these phenotypes could be further assessed by genetic experiments.

In our studies, we used *MIP-Cre/ER* to delete the *Tsc1* gene in pancreatic β-cells. By contrast, others used *Rip-Cre* to generate conditional deletion of *Tsc1* or *Tsc2* in β-cells (Rachdi *et al.* 2008, Shigeyama *et al.* 2008, Mori *et al.* 2009*b*). The *Rip-Cre Tsc1* or *Tsc2* mice showed an increase in islet mass, β-cell size and insulin content at a young age, but *Rip-Cre Tsc1*-knockout mice developed diabetes and β-cell failure after 40 weeks (Rachdi *et al.* 2008, Shigeyama *et al.* 2008, Mori *et al.* 2009*b*). In addition, *Rip-Cre Tsc1*-knockout mice also developed obesity and insulin resistance. In contrast, our mice did not demonstrate effects on body weight, and the knockout mice maintained improved insulin sensitivity at least up to 5 months of age (not shown). These differences could be due at least in part to a functional effect of Tsc1 on the hypothalamus because *Rip-Cre* in contrast to *MIP-Cre* is also expressed in hypothalamus. The genetic background of the mice used may also affect the phenotypes since different genetic backgrounds affect insulin sensitivity and β-cell function (Kahn *et al.* 2012). *Tsc1*$^{F/F}$*Cre*$^{+}$ mice also showed an increase in β-cell proliferation besides cell size, which is consistent with the deletion of *Tsc2* in β-cells (Rachdi *et al.* 2008). However, β-cell proliferation was not altered in the *Rip-Cre Tsc1* KO mice. The results suggest that Tsc1 and Tsc2 may have different function in β-cells and the hypothalamus, although it is generally believed that Tsc1 and Tsc2 function together as a complex. Thus, additional studies are needed to determine precisely how mTORC1 acts upon 4E-BPs and S6K to modulate β-cell mass, proliferation and function.

Previous studies have established important roles of insulin signaling in maintaining β-cell size, proliferation and insulin secretion through regulating multiple pathways, including mTOR. mTOR is essential for cell size and proliferation and is part of two mTOR complexes (mTORC), mTORC1 and 2. mTORC1 activity is negatively regulated by TSC1, TSC2 and the small G protein Rheb (Bond 2016). This pathway integrates signals from growth factors and nutrients and controls growth, proliferation and metabolism by directly modulating 4E-BP and S6 kinases (S6K) and by indirectly attenuating Akt signaling via an mTORC1/S6K-mediated negative-feedback loop on IRS signaling. Tsc1 and Tsc2 mutations specifically activate mTORC1. In this study, we found that insulin expression levels and phosphorylation of AKT were significant decreased in Pdx1 KD MIN6 cells even under IGF-1 stimulation, which may be related to the decreased insulin secretion and insulin content shown in Fig. 7, which is consistent with other studies (Iype *et al.* 2005). Once activated by insulin, AKT can also directly activate mTORC1. In our previous study, Pdx1 deficiency induces an increase in Bim and Puma (Ren *et al.* 2014*a*). Bim is a target of Akt/mTOR signaling. Direct phosphorylation at S87 attenuates Bim's proapoptotic function and is mediated by PKB/Akt (Qi *et al.* 2006). Moreover, the transcription of Bim and Puma is under the negative control of the Akt/mTOR/FoxO axis (Gilley *et al.* 2003, You *et al.* 2006).

In addition, GSK3β is a negative factor for β-cell mass and function. GSk3β deficiency in *Irs2*$^{-/-}$ mice preserved β-cell mass by reversing its negative effects on proliferation

http://joe.endocrinology-journals.org
https://doi.org/10.1530/JOE-18-0015

and apoptosis through increasing Pdx1 (Tanabe *et al.* 2008). Surprisingly, GSK3β was decreased in Pdx1 KD MIN6 cells. The decrease in GSK3β may be the feedback of Pdx1-deficient cells in order to maintain cell survival and proliferation. However, the mechanism for decreased GSK3β in Pdx1 KD cells needs to be further investigated. Thus, the effects of Pdx1 deficiency on mTORC1 activity increased Tsc1 and Tsc2 expressions and decreased AKT activity.

In conclusion, we have shown that Pdx1 deficiency induces a decrease in β-cell size and proliferation. mTORC1 plays an important role in regulating β-cell size and proliferation in Pdx1-deficient β-cells. Genetic ablation of Tsc1 in β-cells increases β-cell size, proliferation and insulin secretion and preserves β-cell mass in *Pdx1*$^{+/-}$ mice. These results suggest Tsc1 and mTORC1 may be targets for therapeutic interventions in diabetes associated with reductions in β-cell mass.

Supplementary data

This is linked to the online version of the paper at https://doi.org/10.1530/JOE-18-0015.

Declaration of interest

The authors declare that there is no conflict of interest that could be perceived as prejudicing the impartiality of the research reported.

Funding

This study was supported by P30-DK020595 (The University of Chicago and Diabetes Research and Training Center).

Author contribution statement

D R designed research; J S, L M, Y H and M L performed research; D R analyzed data; and D R wrote the paper.

Acknowledgements

The authors thank Dr Kenneth Polonsky for insightful suggestions, advice and discussions.

References

Ahlgren U, Jonsson J, Jonsson L, Simu K & Edlund H 1998 beta-Cell-specific inactivation of the mouse Ipf1/Pdx1 gene results in loss of the beta-cell phenotype and maturity onset diabetes. *Genes and Development* **12** 1763–1768. (https://doi.org/10.1101/gad.12.12.1763)

Balcazar N, Sathyamurthy A, Elghazi L, Gould A, Weiss A, Shiojima I, Walsh K & Bernal-Mizrachi E 2009 mTORC1 activation regulates beta-cell mass and proliferation by modulation of cyclin D2 synthesis and stability. *Journal of Biological Chemistry* **284** 7832–7842. (https://doi.org/10.1074/jbc.M807458200)

Blandino-Rosano M, Chen AY, Scheys JO, Alejandro EU, Gould AP, Taranukha T, Elghazi L, Cras-Meneur C & Bernal-Mizrachi E 2012 mTORC1 signaling and regulation of pancreatic beta-cell mass. *Cell Cycle* **11** 1892–1902. (https://doi.org/10.4161/cc.20036)

Bond P 2016 Regulation of mTORC1 by growth factors, energy status, amino acids and mechanical stimuli at a glance. *Journal of the International Society of Sports Nutrition* **13** 8. (https://doi.org/10.1186/s12970-016-0118-y)

Bonner-Weir S, Li WC, Ouziel-Yahalom L, Guo L, Weir GC & Sharma A 2010 Beta-cell growth and regeneration: replication is only part of the story. *Diabetes* **59** 2340–2348. (https://doi.org/10.2337/db10-0084)

Chintinne M, Stange G, Denys B, Ling Z, In 't Veld P & Pipeleers D 2012 Beta cell count instead of beta cell mass to assess and localize growth in beta cell population following pancreatic duct ligation in mice. *PLoS ONE* **7** e43959. (https://doi.org/10.1371/journal.pone.0043959)

Dor Y, Brown J, Martinez OI & Melton DA 2004 Adult pancreatic beta-cells are formed by self-duplication rather than stem-cell differentiation. *Nature* **429** 41–46. (https://doi.org/10.1038/nature02520)

Feng YM, Zhao D, Zhang N, Yu CG, Zhang Q, Thijs L & Staessen JA 2016 Insulin resistance in relation to lipids and inflammation in type-2 diabetic patients and non-diabetic people. *PLoS ONE* **11** e0153171. (https://doi.org/10.1371/journal.pone.0153171)

Fiaschi-Taesch NM, Salim F, Kleinberger J, Troxell R, Cozar-Castellano I, Selk K, Cherok E, Takane KK, Scott DK & Stewart AF 2010 Induction of human beta-cell proliferation and engraftment using a single G1/S regulatory molecule, cdk6. *Diabetes* **59** 1926–1936. (https://doi.org/10.2337/db09-1776)

Fiaschi-Taesch NM, Kleinberger JW, Salim FG, Troxell R, Wills R, Tanwir M, Casinelli G, Cox AE, Takane KK, Srinivas H, *et al.* 2013 Cytoplasmic-nuclear trafficking of G1/S cell cycle molecules and adult human beta-cell replication: a revised model of human beta-cell G1/S control. *Diabetes* **62** 2460–2470. (https://doi.org/10.2337/db12-0778)

Fujimoto K, Chen Y, Polonsky KS & Dorn GW 2nd 2010*a* Targeting cyclophilin D and the mitochondrial permeability transition enhances beta-cell survival and prevents diabetes in Pdx1 deficiency. *PNAS* **107** 10214–10219. (https://doi.org/10.1073/pnas.0914209107)

Fujimoto K, Ford EL, Tran H, Wice BM, Crosby SD, Dorn GW 2nd & Polonsky KS 2010*b* Loss of Nix in Pdx1-deficient mice prevents apoptotic and necrotic beta cell death and diabetes. *Journal of Clinical Investigation* **120** 4031–4039. (https://doi.org/10.1172/JCI44011)

Gilley J, Coffer PJ & Ham J 2003 FOXO transcription factors directly activate bim gene expression and promote apoptosis in sympathetic neurons. *Journal of Cell Biology* **162** 613–622. (https://doi.org/10.1083/jcb.200303026)

Huang J & Manning BD 2008 The TSC1-TSC2 complex: a molecular switchboard controlling cell growth. *Biochemical Journal* **412** 179–190. (https://doi.org/10.1042/BJ20080281)

Iype T, Francis J, Garmey JC, Schisler JC, Nesher R, Weir GC, Becker TC, Newgard CB, Griffen SC & Mirmira RG 2005 Mechanism of insulin gene regulation by the pancreatic transcription factor Pdx-1: application of pre-mRNA analysis and chromatin immunoprecipitation to assess formation of functional transcriptional complexes. *Journal of Biological Chemistry* **280** 16798–16807. (https://doi.org/10.1074/jbc.M414381200)

Jewell JL & Guan KL 2013 Nutrient signaling to mTOR and cell growth. *Trends in Biochemical Sciences* **38** 233–242. (https://doi.org/10.1016/j.tibs.2013.01.004)

Johnson JD, Ahmed NT, Luciani DS, Han Z, Tran H, Fujita J, Misler S, Edlund H & Polonsky KS 2003 Increased islet apoptosis in Pdx1+/- mice. *Journal of Clinical Investigation* **111** 1147–1160. (https://doi.org/10.1172/JCI200316537)

Kahn SE, Suvag S, Wright LA & Utzschneider KM 2012 Interactions between genetic background, insulin resistance and beta-cell function. *Diabetes, Obesity and Metabolism* **14** (Supplement 3) 46–56. (https://doi.org/10.1111/j.1463-1326.2012.01650.x)

Kim YC & Guan KL 2015 mTOR: a pharmacologic target for autophagy regulation. *Journal of Clinical Investigation* **125** 25–32. (https://doi.org/10.1172/JCI73939)

Lee CH, Inoki K & Guan KL 2007 mTOR pathway as a target in tissue hypertrophy. *Annual Review of Pharmacology and Toxicology* **47** 443–467. (https://doi.org/10.1146/annurev.pharmtox.47.120505.105359)

Liu H, Remedi MS, Pappan KL, Kwon G, Rohatgi N, Marshall CA & McDaniel ML 2009 Glycogen synthase kinase-3 and mammalian target of rapamycin pathways contribute to DNA synthesis, cell cycle progression, and proliferation in human islets. *Diabetes* **58** 663–672. (https://doi.org/10.2337/db07-1208)

Meier JJ, Butler AE, Saisho Y, Monchamp T, Galasso R, Bhushan A, Rizza RA & Butler PC 2008 Beta-cell replication is the primary mechanism subserving the postnatal expansion of beta-cell mass in humans. *Diabetes* **57** 1584–1594. (https://doi.org/10.2337/db07-1369)

Mori H, Inoki K, Munzberg H, Opland D, Faouzi M, Villanueva EC, Ikenoue T, Kwiatkowski D, MacDougald OA, Myers MG Jr, *et al*. 2009*a* Critical role for hypothalamic mTOR activity in energy balance. *Cell Metabolism* **9** 362–374. (https://doi.org/10.1016/j.cmet.2009.03.005)

Mori H, Inoki K, Opland D, Munzberg H, Villanueva EC, Faouzi M, Ikenoue T, Kwiatkowski DJ, Macdougald OA, Myers MG Jr, *et al*. 2009*b* Critical roles for the TSC-mTOR pathway in beta-cell function. *American Journal of Physiology: Endocrinology and Metabolism* **297** E1013–E1022. (https://doi.org/10.1152/ajpendo.00262.2009)

Oropeza D, Jouvet N, Budry L, Campbell JE, Bouyakdan K, Lacombe J, Perron G, Bergeron V, Neuman JC, Brar HK, *et al*. 2015 Phenotypic characterization of MIP-CreERT1Lphi mice with transgene-driven islet expression of human growth hormone. *Diabetes* **64** 3798–3807. (https://doi.org/10.2337/db15-0272)

Qi XJ, Wildey GM & Howe PH 2006 Evidence that Ser87 of BimEL is phosphorylated by Akt and regulates BimEL apoptotic function. *Journal of Biological Chemistry* **281** 813–823. (https://doi.org/10.1074/jbc.M505546200)

Rachdi L, Balcazar N, Osorio-Duque F, Elghazi L, Weiss A, Gould A, Chang-Chen KJ, Gambello MJ & Bernal-Mizrachi E 2008 Disruption of Tsc2 in pancreatic beta cells induces beta cell mass expansion and improved glucose tolerance in a TORC1-dependent manner. *PNAS* **105** 9250–9255. (https://doi.org/10.1073/pnas.0803047105)

Ren D, Sun J, Mao L, Ye H & Polonsky KS 2014*a* BH3-only molecule Bim mediates beta-cell death in IRS2 deficiency. *Diabetes* **63** 3378–3387. (https://doi.org/10.2337/db13-1814)

Ren D, Sun J, Wang C, Ye H, Mao L, Cheng EH, Bell GI & Polonsky KS 2014*b* The role of BH3-only molecules Bim and Puma in beta-cell death in Pdx1 deficiency. *Diabetes* **63** 2744–2750. (https://doi.org/10.2337/db13-1513)

Shah OJ, Wang Z & Hunter T 2004 Inappropriate activation of the TSC/Rheb/mTOR/S6K cassette induces IRS1/2 depletion, insulin resistance, and cell survival deficiencies. *Current Biology* **14** 1650–1656. (https://doi.org/10.1016/j.cub.2004.08.026)

Shigeyama Y, Kobayashi T, Kido Y, Hashimoto N, Asahara S, Matsuda T, Takeda A, Inoue T, Shibutani Y, Koyanagi M, *et al*. 2008 Biphasic response of pancreatic beta-cell mass to ablation of tuberous sclerosis complex 2 in mice. *Molecular and Cellular Biology* **28** 2971–2979. (https://doi.org/10.1128/MCB.01695-07)

Shimobayashi M & Hall MN 2014 Making new contacts: the mTOR network in metabolism and signalling crosstalk. *Nature Reviews Molecular Cell Biology* **15** 155–162. (https://doi.org/10.1038/nrm3757)

Stolovich-Rain M, Hija A, Grimsby J, Glaser B & Dor Y 2012 Pancreatic beta cells in very old mice retain capacity for compensatory proliferation. *Journal of Biological Chemistry* **287** 27407–27414. (https://doi.org/10.1074/jbc.M112.350736)

Tanabe K, Liu Z, Patel S, Doble BW, Li L, Cras-Meneur C, Martinez SC, Welling CM, White MF, Bernal-Mizrachi E, *et al*. 2008 Genetic deficiency of glycogen synthase kinase-3beta corrects diabetes in mouse models of insulin resistance. *PLoS Biology* **6** e37. (https://doi.org/10.1371/journal.pbio.0060037)

Uchizono Y, Baldwin AC, Sakuma H, Pugh W, Polonsky KS & Hara M 2009 Role of HNF-1alpha in regulating the expression of genes involved in cellular growth and proliferation in pancreatic beta-cells. *Diabetes Research and Clinical Practice* **84** 19–26. (https://doi:10.1016/j.diabres.2008.12.014)

Wicksteed B, Brissova M, Yan W, Opland DM, Plank JL, Reinert RB, Dickson LM, Tamarina NA, Philipson LH, Shostak A, *et al*. 2010 Conditional gene targeting in mouse pancreatic ss-Cells: analysis of ectopic Cre transgene expression in the brain. *Diabetes* **59** 3090–3098. (https://doi.org/10.2337/db10-0624)

Wittenberg AD, Azar S, Klochendler A, Stolovich-Rain M, Avraham S, Birnbaum L, Binder Gallimidi A, Katz M, Dor Y & Meyuhas O 2016 Phosphorylated ribosomal protein S6 is required for Akt-driven hyperplasia and malignant transformation, but not for hypertrophy, aneuploidy and hyperfunction of pancreatic beta-cells. *PLoS ONE* **11** e0149995. (https://doi.org/10.1371/journal.pone.0149995)

You H, Pellegrini M, Tsuchihara K, Yamamoto K, Hacker G, Erlacher M, Villunger A & Mak TW 2006 FOXO3a-dependent regulation of Puma in response to cytokine/growth factor withdrawal. *Journal of Experimental Medicine* **203** 1657–1663. (https://doi.org/10.1084/jem.20060353)

Received in final form 30 May 2018
Accepted 5 June 2018
Accepted Preprint published online 6 June 2018